Carcinogenesis vol.30 no.3 pp.397–407, 2009
doi:10.1093/carcin/bgp001
Advance Access publication January 6, 2009

Differential roles for membrane-bound and soluble syndecan-1 (CD138) in breast cancer progression

Viktoriya Nikolova, Chuay-Yeng Koo[1], Sherif Abdelaziz Ibrahim, Zihua Wang[2], Dorothe Spillmann[3], Rita Dreier[4], Reinhard Kelsch[5], Jeanett Fischgräbe, Martin Smollich, Laura H.Rossi, Walter Sibrowski[5], Pia Wülfing, Ludwig Kiesel, George W.Yip[1] and Martin Götte*

Department of Gynecology and Obstetrics, University Hospital Münster, D-48149 Münster, Germany, [1]Department of Anatomy, Yong Loo Lin School of Medicine, National University of Singapore, Singapore 117597, [2]Agencourt Biosciences Corporation, Beverly, MA 01915, USA, [3]Department of Medical Biochemistry and Microbiology, The Biomedical Center University of Uppsala, PO Box 582, SE-751 23 Uppsala, Sweden, [4]Department of Physiological Chemistry and Pathobiochemistry and [5]Institute of Transfusion Medicine and Transplantation Immunology, University Hospital of Münster, D-48149 Münster, Germany

*To whom correspondence should be addressed. Tel: +49 251 83 56117; Fax: +49 251 83 55928;
Email: martingotte@uni-muenster.de
Correspondence may also be addressed to George W.Yip. Tel: +65 6516 3206; Fax: +65 6778 7643;
Email: georgeyip@nus.edu.sg

The heparan sulfate proteoglycan syndecan-1 (Sdc1) modulates cell proliferation, adhesion, migration and angiogenesis. Proteinase-mediated shedding converts Sdc1 from a membrane-bound coreceptor into a soluble effector capable of binding the same ligands. In breast carcinomas, Sdc1 overexpression correlates with poor prognosis and an aggressive phenotype. To distinguish between the roles of membrane-bound and shed forms of Sdc1 in breast cancer progression, human MCF-7 breast cancer cells were stably transfected with plasmids overexpressing wild-type (WT), constitutively shed and uncleavable forms of Sdc1. Overexpression of WT Sdc1 increased cell proliferation, whereas overexpression of constitutively shed Sdc1 decreased proliferation. Fibroblast growth factor-2-mediated mitogen-activated protein kinase signaling was reduced following small-interfering RNA (siRNA)-mediated knockdown of Sdc1 expression. Constitutively, membrane-bound Sdc1 inhibited invasiveness, whereas soluble Sdc1 promoted invasion of MCF-7 cells into matrigel matrices. The latter effect was reversed by the matrix metalloproteinase inhibitors *N*-isobutyl-*N*-(4-methoxyphenylsufonyl) glycyl hydroxamic acid and tissue inhibitor of metalloproteinase (TIMP)-1. Affymetrix microarray analysis identified *TIMP-1, Furin and urokinase-type plasminogen activator receptor* as genes differentially regulated in soluble Sdc1-overexpressing cells. Endogenous TIMP-1 expression was reduced in cells overexpressing soluble Sdc1 and increased in those overexpressing the constitutively membrane-bound Sdc1. Moreover, E-cadherin protein expression was downregulated in cells overexpressing soluble Sdc1. Our results suggest that the soluble and membrane-bound forms of Sdc1 play different roles at different stages of breast cancer progression. Proteolytic conversion of Sdc1 from a membrane-bound into a soluble molecule marks a switch from a proliferative to an invasive phenotype, with implications for breast cancer diagnostics and potential glycosaminoglycan-based therapies.

Abbreviations: ADAMs, a disintegrin and metalloproteinases; BSA, bovine serum albumin; FCS, fetal calf serum; FGF, fibroblast growth factor; HS, heparan sulfate; MAPK, mitogen-activated protein kinase; MMP, matrix metalloproteinase; mRNA, messenger RNA; PBS, phosphate-buffered saline; PCR, polymerase chain reaction; PE, phycoerythrin; PMA, phorbol myristate acetate; Sdc1, syndecan-1; siRNA, small-interfering RNA; TIMP, tissue inhibitor of metalloproteinase; uPAR, urokinase-type plasminogen activator receptor; WT, wild-type.

Introduction

The syndecans are a family of four highly conserved cell surface heparan sulfate (HS) proteoglycans, which are expressed in a cell-type- and tissue-specific, developmentally regulated manner (1–3). In the adult, syndecan-1 (Sdc1) is predominantly expressed by epithelial cells and leucocyte subpopulations. Moreover, its expression can be induced in a variety of cell types during development, wound repair and tumor progression (1,3,4). The Sdc1 core protein contains highly conserved transmembrane and cytoplasmic domains, which mediate oligomerization and interact with the cytoskeleton (1,5–7). The extracellular domain harbors attachment sites for HS, as well as chondroitin sulfate chains (1,3), which are linear polymers of repetitive disaccharide units of uronic acids and variably sulfated *N*-acetylglucosamine (HS) or *N*-acetylgalactosamine (chondroitin sulfate), capable of forming specific ligand-binding motifs (1,8). The HS chains are considered the major functional extracellular domain of Sdc1, whereas few functions have been assigned to the extracellular protein moiety (9–11). Ectodomain shedding reduces the number of surface receptors, thus downregulating signal transduction, converting membrane-bound Sdc1 into a soluble effector competing for the same ligands. Protein kinase C, protein tyrosine kinase and mitogen-activated protein kinase (MAPK) signal transduction pathways activate shedding, which is mediated by several metalloproteinases in a context-dependent manner (1,10,12).

Sdc1 modulates numerous biological processes relevant to tumor progression. Sdc1 is a classical coreceptor for growth factors, angiogenic factors and chemokines (1,3,8) and acts as a cell and matrix adhesion receptor (1,3). In concert with integrins, Sdc1 influences cell spreading and motility (13,14) and modulates protease activities and chemokine functions during inflammation and wound repair (2,3,15,16). An engagement of Sdc1 in angiogenesis has been suggested in different mouse models and in clinical correlation studies (2,3,17–19). Sdc1-deficient mice are resistant to induced breast cancer due to a cancer stem cell phenotype, further underlining its relevance for breast cancer progression (4,8,20).

A prognostic value for Sdc1 expression was assigned in several cancer types, including breast cancer (8). High Sdc1 expression has a predictive value for the response to neoadjuvant chemotherapy of primary breast cancer (21). A study on 254 breast carcinoma cases correlated strong epithelial Sdc1 expression in 42% of the carcinomas with negative prognostic parameters (22). A different study on 200 patients showed a significantly reduced 10 years of breast cancer-specific overall survival for patients displaying epithelial Sdc1 expression and estrogen receptor (ER)-negative status or stromal Sdc1 expression and ER-positive status (23). In contrast, a study on 80 invasive ductal carcinoma patients indicated a loss of epithelial Sdc1 expression correlating with relapse-free survival (24). These data strongly suggest important roles for Sdc1 in breast cancer progression; however, its exact function is still unknown, hampering efficient glycosaminoglycan-targeting therapies (8). We hypothesized that some controversial clinical findings may be due to opposing functions of membrane-bound and shed Sdc1. Therefore, we studied the individual contributions of membrane-bound and soluble Sdc1 to breast cancer cell proliferation and invasiveness *in vitro*. Our findings confirm a differential role of both Sdc1 forms in the modulation of fibroblast growth factor (FGF)-2-mediated MAPK signaling, E-cadherin expression and protease activity.

Materials and methods

Materials

Media, fetal calf serum (FCS) and tissue culture supplies were from Gibco BRL (Karlsruhe, Germany). Unless stated otherwise, all chemicals were from Sigma (Deisenhofen, Germany).

Cell culture

The human breast cancer cell line MCF-7 was maintained in RPMI 1640 containing 10% FCS, 1% glutamine and 1% penicillin–streptomycin (19) in a humidified atmosphere of 5% CO_2 at 37°C. Sdc1 shedding was induced by treatment with 1 μM phorbol myristate acetate (PMA) (Calbiochem, La Jolla, CA) in serum-free medium for 15 min (10).

Generation of stably transfected cell lines

pcDNA3.1-based plasmids (Invitrogen, Karlsruhe, Germany) overexpressing a wild-type (WT), a constitutively membrane-bound (Sdc1-388UC) and a constitutively shed form (Sdc1-392CS) of murine Sdc1 have been described previously (10). Stable MCF-7 cell transfection was performed using lipofectamine (Invitrogen) according to the manufacturer's instructions. After 48 h, cells were split and cultured in the presence of 1 mg/ml G418 to select for clones containing the plasmids. Neomycin-resistant clones were cultured in the presence of 800 μg/ml G418.

Cell proliferation assay

Basal cell proliferation was evaluated using the indicator dye Alamar Blue (Biosource, Camarillo, CA). A total of 2.5×10^3 cells per well were plated in triplicate in 96-well plates and cultured at 37°C for 48 h. Dye was added, and the colorimetric change was measured photometrically after 6 h according to the manufacturer's protocol. The median absorbance values of at least three independent experiments were used for statistical analysis.

Invasion assay and matrix metalloproteinase inhibitor treatments

Twenty-five thousand cells in 0.5 ml RPMI/10% FCS were added in triplicates to the upper compartments of BioCoat Matrigel Invasion Chambers (BD Biosciences, Heidelberg, Germany). After 24 h, the medium was replaced by serum-free RPMI. To the lower compartment, 0.75 ml RPMI/20% FCS was added. After 48 h, the cells on the lower surface were fixed and stained with Diff-Quik dye (Medion, Duedingen, Switzerland). Excised and mounted filter membranes were photographed using a Zeiss Axiovert microscope equipped with Axiovision software (Zeiss, Jena, Germany) at ×100 magnification. For each membrane, cells in five visual fields were counted. Relative invasiveness was expressed as percentage of the cell number on compound-treated inserts compared with control inserts ($n > 3$). For matrix metalloproteinase (MMP) inhibitor studies, the following inhibitors were added to both compartments 24 h after cell plating: 3.5 nM tissue inhibitor of metalloproteinase (TIMP)-1 (Biomol, Hamburg, Germany), 10 nM TIMP-2 (Calbiochem), 1 μM (2R)-2-[(4-biphenylylsulfonyl)amino]-3-phenylpropionic acid (MMP-2/MMP9 inhibitor, Calbiochem), 1.5 and 15 μM *N*-isobutyl-*N*-(4-methoxyphenylsulfonyl) glycyl hydroxamic acid (Biomol).

Immunocytochemistry

Ten thousand cells per well were grown for 16 h in eight-well chamber slides (Nunc, Wiesbaden, Germany). For Sdc1/vinculin colocalization experiments, chamber slides were precoated with 10 μg/ml fibronectin (BD Biosciences). Cells were fixed with either ice-cold methanol (muSdc1/huSdc1) or 3.7% phosphate-buffered saline (PBS)-buffered formaldehyde (muSdc1/vinculin) and permeabilized with 0.1% Triton X-100 in PBS. Non-specific binding was blocked with PBS containing 1% Aurion BSA-c (DAKO, Glostrup, Denmark). Slides were subsequently incubated with rat-anti-mouse Sdc1 mAb 281-2 [BD Pharmingen, San Jose, CA, 1:1000 in PBS/1% bovine serum albumin (BSA)] and mouse-anti-human Sdc1 mAb (Serotec, Martinsried, Germany, 1:100) or mouse-anti-human vinculin mAb (Sigma, 1:250) overnight at 4°C. Primary antibody omission served as a negative control. Subsequently, samples were incubated for 1 h with ALEXA-Fluor-568-labeled goat-anti-rat IgG and ALEXA-Fluor-488 goat-anti-mouse IgG (both Invitrogen, 1:600 in PBS/1% BSA). Cell nuclei were visualized by 4′,6-diamidino-2-phenylindole staining. Slides were analyzed with a Leica DMLB fluorescence microscope equipped with a Leica DC300F camera (muSdc1/huSdc1) or with a Nikon PCM 2000 confocal microscope (muSdc1/vinculin) (Nikon, Düsseldorf, Germany). Images obtained using different fluorescence channels were merged using Adobe Photoshop 6.0 software.

Dot blot analysis

A total of 5×10^5 transfected MCF-7 cells were seeded in six-well plates and cultured for 24 h in the presence of FCS. The medium was subsequently replaced by serum-free medium for 24 h. Cells were lysed in radioimmunoprecipitation buffer and protein content was determined by bicinchoninic acid assay (Pierce, Rockford, IL). Two hundred microliters of cleared (10 000*g*, 4°C, 10 min) cell culture supernatants were loaded on nitrocellulose membranes using a microfiltration apparatus (Bio-Rad, Hercules, CA). Membranes were blocked (15) and incubated for 16 h with the Sdc1 antibody 281-2 (1:100 in PBS/1% BSA) at 4°C. Immunoreactivity was visualized with a peroxidase-conjugated anti-rat-IgG antibody (Oncogene, Cambridge, MA, 1:1000) followed by an enhanced chemoluminescence reaction (SuperSignal, Pierce) and enhanced chemoluminescence-hyperfilm exposure (Amersham, Braunschweig, Germany). Digitalized images were analyzed densitometrically using ImageJ software (National Institutes of Health, Bethesda, MD), normalizing to protein content.

siRNA-treatment and western blot analysis

siRNA knockdown was performed using an equimolar mixture of siRNAs #12527 and #12432 (Ambion, Cambridgeshire, UK) targeting the coding region of Sdc1 and a negative control siRNA (#301698, Qiagen, Hilden, Germany). MCF-7 cells were transfected with 40 nM siRNA using Dharmafect reagent (Dharmacon, Lafayette, CO) according to the manufacturer's instructions. Knockdown was confirmed by quantitative real-time polymerase chain reaction (PCR) and flow cytometry (see below). To analyze MAPK activation, Sdc1-silenced and control MCF-7 cells were serum starved for 48 h prior to stimulation ± 10 nM FGF-2 (R&D systems, Wiesbaden, Germany) for 10 min. Cell lysates were prepared using modified radioimmunoprecipitation buffer with proteinase inhibitors (25). Thirty micrograms of protein per lane were separated on 12% gels and electrotransferred to Hybond nitrocellulose membranes (Amersham). Detection of phosphorylated p44/42-MAPK was performed using a rabbit polyclonal antibody (phospho-Thr202/Tyr204, Cell Signaling, Beverly, MA) diluted 1:1000 and horseradish peroxidase-conjugated anti-rabbit IgG (Cell Signaling, 1:2000). Subsequently, membranes were subjected to an enhanced chemoluminescence reaction and signal quantification with NIH ImageJ software, normalizing the densitometric values of phospho-MAPK to the total MAPK signal. For total MAPK detection, membranes were stripped with glycine buffer (pH 2.5), washed and reincubated with primary antibodies against p44/42-MAPK (Cell Signaling) followed by the procedure described above (25). Urokinase-type plasminogen activator receptor (uPAR), furin, murine Sdc1 and human Sdc1 were detected analogously using rabbit-anti-uPAR (Santa Cruz Biotechnology, Santa Cruz, CA, 1:800), rabbit-anti-furin (Santa Cruz, 1:200), rat-anti-murine Sdc1 clone 281-2 (1:1000) and goat-anti-human Sdc1 (R&D systems, 1:1000) as primary antibodies.

Flow cytometry

Cells were harvested from culture flasks by incubation with 1.5 mM ethylenediaminetetraacetic acid in Ca/Mg-free PBS buffer for 10 min at 37°C with gentle agitation. Cells were washed in PBS and resuspended in cold buffer containing 1% FCS. A total of 2×10^5 cells per sample were used for a single analysis. Following centrifugation, cells were resuspended in Hanks' balanced salt solution/2% BSA and incubated for 15 min at 25°C with titrated antibodies [phycoerythrin (PE) rat IgG2a, κ-isotype control clone R35-95 'R-IgG-PE', 0.1 μg and PE rat-anti-mouse CD138 clone 281-2 'RAM CD138-PE', 0.1 μg (both BD Pharmingen); IOTest Anti-CD138-PC5 clone B-A38 'MAH-CD138-PC5', 3 μl and IOTest IgG1 (mouse) clone 679.1Mc7 'M-IgG-PC5', 3 μl (both Beckman Coulter, Fullerton, CA)]. The samples were analyzed using a Beckman Coulter FC500 flow cytometer. Murine Sdc1 expression was analyzed comparing the relative amount of mouse or human CD138-stained cells with the IgG-controls in transfected and non-transfected cells. Isotype-matched antibodies were used as negative controls and <2% non-specific background staining was observed (c.f. supplementary Figure 2, available at *Carcinogenesis* Online, for details).

TIMP-1 enzyme-linked immunosorbent assay

Fifty microliters of cell culture supernatant from the upper chamber of matrigel invasion assays was analyzed using the Quantikine human TIMP-1 immunoassay (R&D systems) as described by the manufacturer.

Quantitative real-time PCR

Cellular RNA was isolated using the RNeasy kit (Qiagen) and transcribed into complementary DNA applying the Advantage RT-for-PCR-Kit (Clontech, Heidelberg, Germany). Quantitative PCR was performed using the Qiagen QuantiTect SYBR Green PCR kit in a LightCycler (Roche, Indianapolis, IN) as described previously (26). Amplification specificity was verified using melting curve analysis and 2% agarose gel electrophoresis of the PCR products. Data were analyzed using the $2^{-\Delta\Delta Ct}$ method after normalization to glyceraldehyde 3-phosphate dehydrogenase (GAPDH). Primer sequences are listed in Table I.

Microarray expression analysis

Total RNA was isolated from three biological replicates of Sdc1-392CS-transfected and control MCF-7 cells using the RNeasy kit (Qiagen). Preparation of biotin-labeled complementary RNA using the one-cycle labeling protocol, hybridization and scanning of the arrays was performed according to the manufacturer's instructions. A total of 3.6 μg of purified RNA and poly-A controls were used to generate complementary DNA, which was used to synthesize biotin-labeled complementary RNA. Fragmented complementary RNA was hybridized to Human Genome U133 Plus 2.0 arrays for 16 h at 60°C in a GeneChip Hybridization Oven 640 at 60 r.p.m. The arrays were washed and stained in a GeneChip Fluidics 450 station (Affymetrix, Santa Clara, CA),

Table I. Quantitative real-time PCR analysis of gene expression in control MCF-7 cells and MCF-7 cells overexpressing soluble Sdc1

Gene	Gene product (functional classification)	Primer sequence	Relative expression Sdc1-392CS versus control	*P*-value
TIMP-1	TIMP-1	Forward: 5′-TGACATCCGGTTCGTCTACA-3′; reverse: 5′-TGCAGTTTTCCAGCAATGAG-3′	0.1552	0.0018
PLAUR	uPAR (modulation of proteolysis)	Forward: 5′-GCCTTACCGAGGTTGTGTGT-3′; reverse: 5′-CATCCAGGCACTGTTCTTCA-3′	4.9460	0.0233
FURIN	Furin (MMP-processing protease)	Forward: 5′-GAAGTGCACGGAGTCTCACA-3′; reverse: 5′-CCGCCATGTGAGGTTCTTAT-3′	0.4636	0.0213
Hs_SDC1	Sdc1 (human)	Forward: 5′-GGGACTCAGCCTTCAGACAG-3′; reverse: 5′-CTCGTCAATTTCCAGGAGGA-3′	0.2840	0.0033
Mm_SDC1	Sdc1 (murine)	Forward: 5′-GCTCTGGGGATGACTCTGAC-3′; reverse: 5′-AAAGCAGTCTCGGTGTTGCT-3′	9.77×10^5	<0.0001
HPA1	Heparanase (proinvasive heparan sulphate-degrading enzyme)	Forward: 5′-CCTTGCCACCTTTAATGGAA-3′; reverse: 5′-AAGCAGCAACTTTGGCATTT-3′	0.3360	n.s.
CDH	E-cadherin (cell adhesion molecule)	Forward: 5′-TGCCCAGAAAATGAAAAAGG-3′; reverse: 5′-GTGTATGTGGCAATGCGTTC-3′	1.4040	n.s.
MT1-MMP	MT1-MMP (Sdc1-shedding MMP)	Forward: 5′-GCAGAAGTTTTACGGCTTGC-3′; reverse: 5′-TAGCGCTTCCTTCGAACATT-3′	0.308	n.s.
MET	c-Met (hepatocyte growth factor receptor)	Forward: 5′-AAGAGGGCATTTTGGTTGTG-3′; reverse: 5′-GATGATTCCCTCGGTCAGAA-3′	0.4192	n.s.
ITGAV	Integrin alphaV	Forward: 5′-TTCTTCCGATTCCAAACTGG-3′; reverse: 5′-TGCCTTGCTGAATGAACTTG-3	0.7941	n.s.
ITGB5	Integrin beta5	Forward: 5′-GTCAGGAAGGGTCGGAGTCT-3′; reverse: 5′-ACACCTGTGTGCAAGGCATA-3′	0.8211	n.s.
RHOB	RhoB (small guanosine triphosphatase involved in modulating actin cytoskeleton)	Forward: 5′-CTCTGCCAAGACCAAGGAAG-3′; reverse: 5′-CTCATAGCACCTTGCAGCAG-3′	2.1560	n.s.
CDC42	Cdc42 (small guanosine triphosphatase involved in modulating actin cytoskeleton)	Forward: 5′-ACGACCGCTGAGTTATCCAC-3′; reverse: 5′-CCCAACAAGCAAGAAAGGAG-3′	2.0210	n.s.
MAP2K5	MAPK kinase 5	Forward: 5′-ACGTGAAGCCCTCCAATATG-3′; reverse: 5′-GGCGCCATATAAGCATTTGT-3′	1.7430	n.s.
MAP3K8	MAPK kinase kinase 8	Forward: 5′-GTCTGGACTCTGCCCTCTTG-3′; reverse: 5′-GCCGAGGTCGATGTAGAGAG-3′	4.8810	n.s.
GAPDH	GAPDH (housekeeping gene used for PCR data normalization)	Forward: 5′-GAAGGTGAAGGTCGGAGTCAACG-3′; reverse: 5′-TGCCATGGGTGGAATCATATTGG-3′	n.a.	n.a.

n.s., not significant ($P \geq 0.05$); n.a., not applicable.

followed by scanning using an Affymetrix GeneChip Scanner 3000. The raw data image was processed with GeneChip Operating Software v1.2 and analyzed using DNA-Chip Analyzer (27). Cell intensity files were normalized to overall median intensity and expression values were calculated using a perfect match minus mismatch model. The Database for Annotation, Visualization and Integrated Discovery 2008 was used to verify the annotations of the filtered genes ($n = 396$) and classify the genes into different ontology groups.

HS disaccharide analysis

Confluent cell monolayers were washed twice with ice-cold PBS, harvested by cell scraping, pelleted and washed before lyophilization. HS was isolated and digested essentially as described before by proteolytic digestion, nucleic acid removal and removal of chondroitin sulfate before digestion with heparin lyases (28). Sample cleanup after chondroitinase digestion was achieved by passage over diethylaminoethyl anion exchange columns, eluted with 1 M NaCl and desalted before digestion with 50 mU chondroitinase ABC (Seikagaku, Tokyo, Japan) in 100 µl of 40 mM Tris–acetate, pH 8, before repeated cleanup on diethylaminoethyl columns. The samples were then digested with 0.4 mU each of heparin lyases I–III (IBEX, Montreal, Canada) in 100 µl of heparin lyase buffer (5 mM *N*-2-hydroxyethylpiperazine-*N*′-2-ethanesulfonic acid, pH 7, and 1 mM $CaCl_2$) and incubated for 16 h at 37°C. Heat-inactivated digests were loaded for analysis by reversed-phase ion-pair chromatography–high-performance liquid chromatography as described (28).

Statistical analysis

Data were expressed as mean ± SEM or SD, as indicated. Statistical analysis was performed using the Sigma Stat 3.1 software (Systat Software, Point Richmond, CA). An unpaired *t*-test was used when groups passed the normality test, and a Mann–Whitney test was used when the standard deviations of two groups differed significantly. A two-sided *P*-value <0.05 was considered statistically significant. All calculations were performed on the means of triplicate-sextuplet measurements of at least three independent experiments.

Results

Heterologous overexpression of constitutively shed and constitutively membrane-bound Sdc1 in MCF-7 breast cancer cells

To evaluate a potential differential role of membrane-bound and soluble Sdc1 on breast cancer cell behavior, we employed a stable transfection approach in MCF-7 breast cancer cells. Expression construct Sdc1-392CS encodes only the extracellular domain of Sdc1, whereas construct Sdc1-388UC allows for overexpression of an uncleavable, constitutively membrane-bound form in which the juxtamembrane shedding site is replaced by CD4 sequences (10). Endogenously expressed human and overexpressed murine Sdc1, which share 70% amino acid sequence identity in their extracellular and 96 and 100% homology in their cytoplasmic and transmembrane domains (29), can be distinguished using species-specific reagents. Functional equivalence of murine and human Sdc1 was demonstrated in several studies (29,30). MCF-7 cells were stably transfected with a pcDNA3.1 control vector, a pcDNA3.1-based Sdc1-WT, Sdc1-392CS and Sdc1-388UC constructs. A series of control experiments were performed to demonstrate overexpression, proper location and glycosaminoglycan substitution of the Sdc1 constructs. A significant level of messenger RNA (mRNA) overexpression was demonstrated for the heterologous constructs by real-time PCR (Figure 1A). Soluble ectodomain overexpression resulted in a 60% decrease of endogenous Sdc1 expression, whereas overexpression of WT and constitutively membrane-bound Sdc1 did not affect endogenous Sdc1 levels (Figure 1A). Dot blot analysis revealed 5-fold increased murine Sdc1 levels in Sdc1-392CS compared with Sdc1-WT conditioned media (Figure 1B). Using immunofluorescence microscopy, the colocalization of

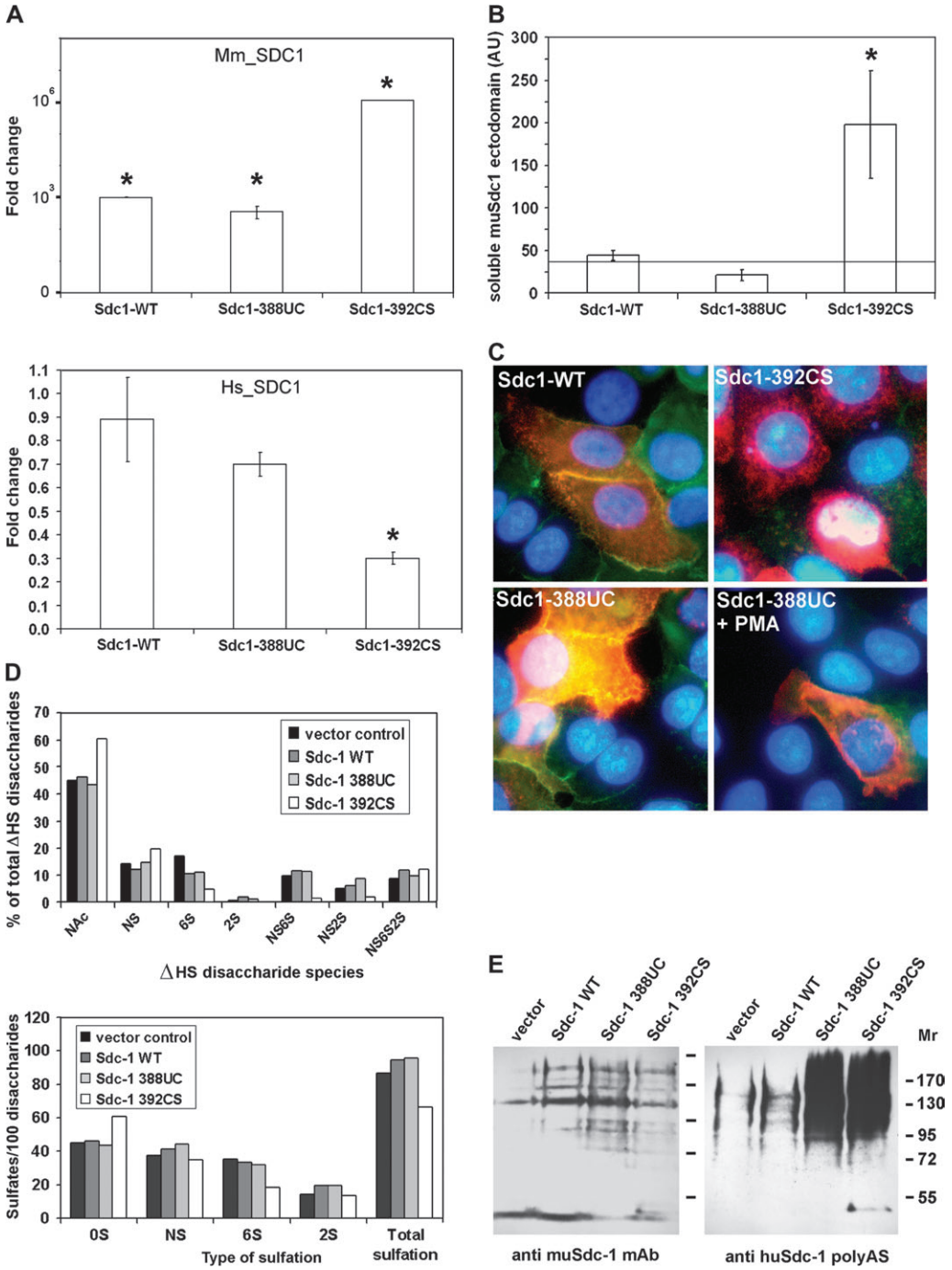

Fig. 1. Heterologous overexpression of Sdc1 constructs encoding WT murine Sdc1 (Sdc1-WT), an uncleavable Sdc1 construct resistant to MMP-mediated shedding (Sdc1-388UC) or a constitutively shed soluble ectodomain construct (Sdc1-392CS) in stably transfected MCF-7 breast cancer cells. (**A**) Quantitative PCR analysis of murine (Mm_SDC1, upper panel) and human (Hs_SDC1, lower panel) Sdc1 expression. Data are expressed as fold change versus control vector-transfected MCF-7 cells. $^{*}P < 0.05$, $n \geq 3$, error bars = SEM. (**B**) Dot blot analysis for heterologous Sdc1 ectodomain expression in conditioned media of the stably transfected cell lines. Horizontal line = background signal in vector control MCF-7 cells. $^{*}P < 0.05$, $n = 3$, error bars = SEM. (**C**) Coimmunolocalization of endogenous and heterologously expressed Sdc1. Stably transfected MCF-7 cells were processed for immunostaining with monoclonal antibodies against human (green fluorescent secondary antibody) and murine (red fluorescent secondary antibody) Sdc1 as described in Materials and Methods. Yellow color denotes Sdc1 colocalization and blue color denotes 4′,6-diamidino-2-phenylindole nuclear staining. Like endogenous Sdc1, overexpressed Sdc1-WT and Sdc1-388UC show a largely membranous staining. No membranous staining is observed for the constitutively shed Sdc1-392CS construct. The uncleavable Sdc1-388UC construct retains its membrane location even after exposure to 1 μM PMA, a strong inducer of Sdc1 shedding (10). (**D**) HS disaccharide analysis of the cell lines employed in this study. HS was isolated from the indicated cell lines and products were exhaustively digested with a mixture of heparin lyases (see Materials and Methods). Upper panel: the disaccharide products containing non-reducing-terminal 4,5-unsaturated hexuronic acid residues (ΔHexA) were analyzed by reversed-phase ion-pair chromatography–high-performance liquid chromatography, as described in Materials and Methods. The disaccharide composition is indicated with *N*-acetylglucosamine (NAc), *N*-sulfated glucosamine (NS) and sulfate group at indicated position (S). Lower panel: overall sulfate contents (total sulfation), specified according to the type of substituent as non-sulfated (OS), total *N*-sulfated (NS), total 6-*O*-sulfated (6S) and total 2-*O*-sulfated disaccharides (2S). (**E**) Western blot of MCF-7 transfectant extracts with the monoclonal antibody 281-2 directed against murine Sdc1 (anti-muSdc1 mAb) and a polyclonal rabbit antiserum directed against human Sdc1 (anti-huSdc1 poly-AS). Western blotting reveals the presence and overexpression of the glycosaminoglycan-substituted forms (80–190 kDa) of murine Sdc1. Due to the extensive sequence homology of muSdc1 and huSdc1, a slight crossreactivity of the antibodies is observed. Mr = migration position of molecular weight standards.

endogenous and heterologously overexpressed Sdc1 was studied (Figure 1C; supplementary Figure 1 is available at *Carcinogenesis* Online). Similar to endogenous Sdc1 expression in breast cancer cells (M.Götte, unpublished data), heterologously expressed Sdc1 showed variable expression levels. Both WT forms of Sdc1 colocalized at the cell surface (Figure 1C panel Sdc1-WT), as independently confirmed by flow cytometry (supplementary Figure 2 is available at *Carcinogenesis* Online). Occasionally, an additional perinuclear or nuclear localization of Sdc1 was observed. In contrast to WT Sdc1, the constitutively shed form was detected intracellularly only (Figure 1C panel Sdc1-392CS) since soluble extracellular Sdc1 may have been washed out during the staining procedure. However, cell-associated soluble Sdc1 could be detected by flow cytometry, possibly due to secondary HS-mediated association with cell surface receptors (supplementary Figure 2 is available at *Carcinogenesis* Online). MCF-7 Sdc1-392CS cells showed a more rounded morphology compared with vector controls (Figure 1C panel Sdc1-392CS). A potential downregulation of endogenous Sdc1 protein expression, as suggested by mRNA expression data and conventional immunostainings (Figure 1C panel Sdc1-392CS), could not be confirmed by confocal immunofluorescence microscopy and flow cytometry (supplementary Figures 1 and 2 are available at *Carcinogenesis* Online). The constitutively membrane-bound form showed a prominent membrane localization (Figure 1c panel Sdc1-388UC). Flow cytometric analysis confirmed cell surface localization, reaching ~60% of the mean fluorescence intensity of the Sdc1-WT construct (supplementary Figure 2 is available at *Carcinogenesis* Online). Treatment of MCF-7 Sdc1-388UC cells with PMA did not result in induced cleavage of the Sdc1-388UC mutant, whereas endogenous Sdc1 was shed following this treatment (Figure 1C panel Sdc1-388UC), demonstrating functionality of the Sdc1-388UC 'uncleavable' construct (10). Since the HS chains represent the major functional extracellular domain of Sdc1, we analyzed the transfectants for glycosaminoglycan substitution of heterologously expressed Sdc1 and for possible changes in HS structure. A disaccharide analysis of the transfected cells did not reveal major differences in HS composition, except for a reduced sulfation degree in Sdc1-392CS-overexpressing cells (Figure 1D). Western blotting analysis of cell extracts for the expression of murine and human Sdc1 confirmed glycosaminoglycan substitution of both human and murine Sdc1, as revealed by the presence of high-molecular weight (80–190 kDa) bands (Figure 1E).

Differential effect of soluble and membrane-bound Sdc1 on breast cancer cell proliferation

Sdc1 acts as a membrane-bound coreceptor for FGF receptor-mediated signaling (31). However, soluble Sdc1 ectodomains can competitively inhibit heparin-mediated FGF-2 mitogenicity (29,32,33). To characterize the role of endogenous Sdc1 in MCF-7 cell proliferation, we studied its function in FGF-2-mediated MAPK signaling as a downstream readout of FGF receptor activity. siRNA knockdown resulted in an 80% downregulation of endogenous Sdc1 expression in MCF-7 cells 48 h after transfection, as confirmed by quantitative PCR and flow cytometry (Figure 2A and B). FGF-2 stimulation of serum-starved MCF-7 cells induced p44/42 MAPK phosphorylation, which could be significantly reduced by Sdc1 siRNA knockdown (Figure 2C). Proliferation assays revealed significantly increased proliferation rates in MCF-7 cells overexpressing WT Sdc1 compared with vector controls (Figure 2D). In contrast, overexpression of soluble Sdc1 inhibited MCF-7 breast cancer cell proliferation (Figure 2D).

The soluble Sdc1 ectodomain promotes breast cancer cell invasiveness via a TIMP-1-dependent mechanism

Sdc1 acts as a matrix receptor and as a modulator of cell motility and of the proteolytic environment, key elements of the metastatic process (1,8,11). We therefore investigated if MCF-7 cell invasiveness was differentially affected by overexpression of the soluble ectodomains, constitutively membrane-bound or WT Sdc1 using matrigel invasion chamber assays. Overexpression of WT Sdc1 increased MCF-7 cell invasiveness by 50% compared with vector controls (Figure 3A). Overexpression of the soluble Sdc1 ectodomain led to a 130% increase, whereas constitutively membrane-bound Sdc1 overexpression entailed a 40% decrease of invasiveness (Figure 3A). Since Sdc1 modulates the activity of a variety of proteases, with potentially opposing physiological effects of the soluble and membrane-bound form (2,30,34,35), we tested if MMP inhibitors would differentially reduce invasiveness. *N*-isobutyl-*N*-(4-methoxyphenylsulfonyl) glycyl hydroxamic acid, an MMP inhibitor with broad specificity (36–38), inhibited MCF-7 Sdc1-392CS invasiveness by 50%; however, it did not influence invasiveness of the other transfectants. The physiological inhibitor TIMP-1 inhibited MCF-7 Sdc1-392CS invasion by 40% and MCF-7 Sdc1-388UC invasion by >50%, whereas TIMP-2 and an MMP2/MMP9 inhibitor had no effect (Figure 3B–E).

Affymetrix microarray analysis for differential gene expression in MCF-7 control cells and MCF-7 cells overexpressing soluble Sdc1

Since Sdc1 modulates both expression and function of many factors relevant to cancer cell invasion and metastasis (8), we performed an Affymetrix microarray analysis to screen for genes differentially expressed between low-invasive MCF-7 vector control and highly invasive MCF-7 Sdc1-392CS cells. Relative to controls, 59 genes were significantly upregulated and 330 genes downregulated in cells overexpressing soluble Sdc1 by at least a factor of two (Figure 4A; supplementary Tables I and II are available at *Carcinogenesis* Online). Differentially regulated genes were placed into categories based on their Gene Ontology annotations (39), and candidate groups of genes potentially involved in the observed phenotypic changes in MCF-7 392CS cells were subjected to further analysis (Figure 4B; supplementary Table III is available at *Carcinogenesis* Online). Microarray analysis revealed a significant downregulation of *TIMP-1*. Quantitative PCR confirmed significant downregulation of *TIMP-1* mRNA and upregulation of *uPAR* in MCF-7 Sdc1-392CS cells, providing clues for a proinvasive mechanism induced by soluble Sdc1 (Table I). Expression changes affecting members of the Rho family of small guanosine triphosphatases and of integrin alphaV and beta5 subunits indicated that changes in cell motility might have caused increased invasiveness in MCF-7 Sdc1-392CS cells. However, quantitative PCR analysis (Table I) and western blotting (results not shown) could not confirm differential expression of *RhoB* and β*5-integrin* and of additional proinvasive factors like the hepatocyte growth factor receptor cMet or heparanase (8,19). Moreover, confocal immunofluorescence microscopy indicated that all cell lines were capable of forming focal adhesions (Figure 4C; supplementary Figure 1 is available at *Carcinogenesis* Online).

Overexpression of the soluble Sdc1 ectodomain induces downregulation of TIMP-1 and E-cadherin and increased uPAR expression

We next aimed at confirming the results of Affymetrix screening and real-time PCR analysis at the protein level. Since *TIMP-1* mRNA expression was downregulated in MCF-7 Sdc1-392CS cells, we determined TIMP-1 protein in cell culture supernatants of all four transfectant cell lines by enzyme-linked immunosorbent assay. TIMP-1 levels were significantly decreased in cells overexpressing soluble Sdc1, whereas increased TIMP-1 amounts were detected in the media of cells overexpressing constitutively membrane-bound Sdc1 (Figure 5A). While E-cadherin mRNA expression was not significantly altered in MCF-7-Sdc1-392CS cells (Table I), western blot analysis revealed significant downregulation of E-cadherin protein expression compared with controls (Figure 5B). Expression of the uPAR in MCF-7 cells overexpressing soluble Sdc1 was significantly upregulated at both mRNA and protein levels (Figure 5C). In contrast, transcriptional downregulation of the proprotein convertase furin did not translate into changes in protein expression (Figure 5D).

Discussion

In this study, we employed an overexpression approach to delineate the role of membrane-bound and soluble forms of Sdc1 in breast cancer cell behavior. We confirmed the correct localization and

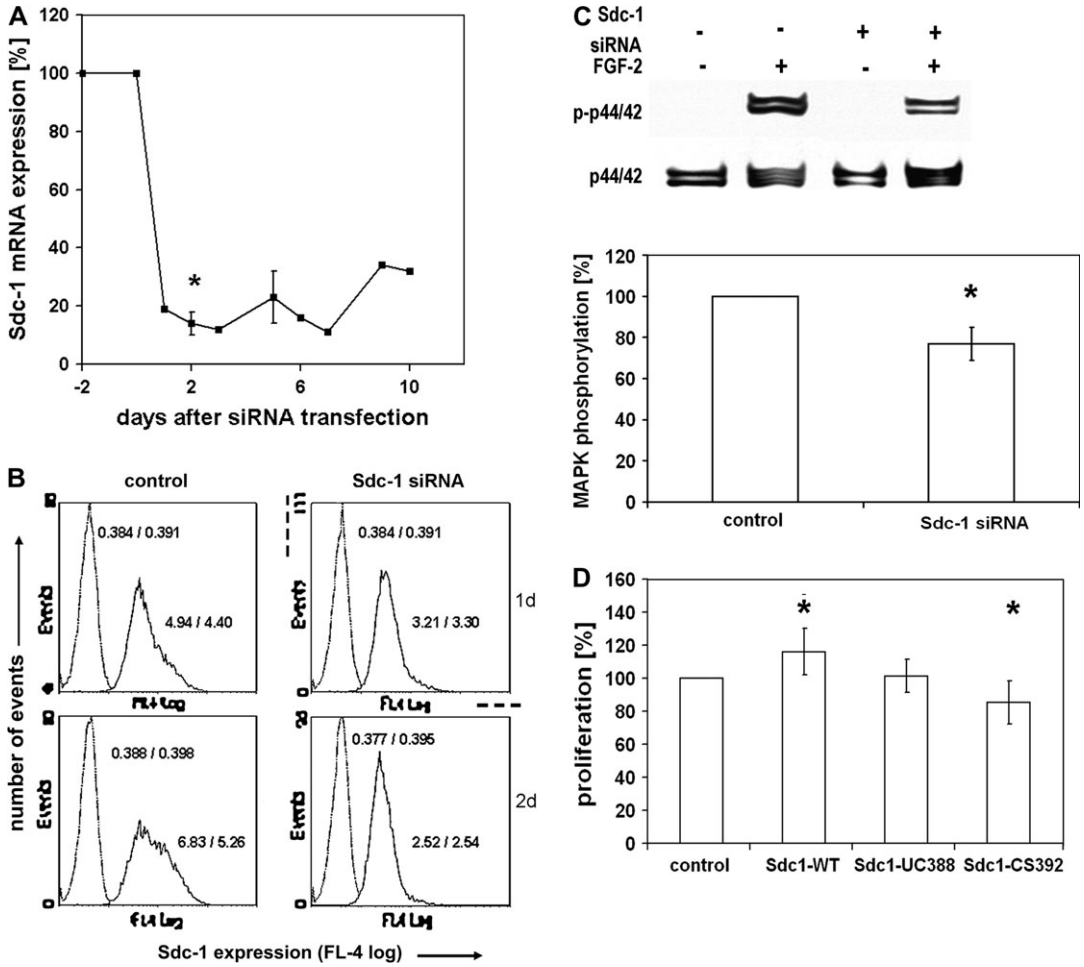

Fig. 2. Sdc1 modulates FGF-2-mediated MAPK signaling and proliferation in MCF-7 breast cancer cells. (**A**) siRNA-mediated knockdown of endogenous Sdc1 mRNA expression in MCF-7 cells at indicated time points ($P < 0.05$, $n = 5$ for 48 h, $n = 2$ for other timepoints, error bars = SD). (**B**) Flow cytometric analysis of siRNA-mediated Sdc1 knockdown in MCF-7 cells. Each plot shows MS-IgG-PC5 control (dotted line) and MAH-CD138-PC5-stained cells (solid line). The median fluorescence intensity is given for each peak (two values from repeated measurements, plots from first measurement). (**C**) Western blot analysis of FGF-2-mediated p44/42 MAPK activation in Sdc1-silenced MCF-7 cells. MCF-7 cells were transfected with a control siRNA or a Sdc1 siRNA construct and serum-starved for 24 h after transfection. Cells were treated ± 10 nM FGF-2 for 10 min, lysed and analyzed by western blotting as described. Upper panel: representative blotting result; lower panel: densitometric analysis of five individual experiments. $^{*}P < 0.05$, $n = 5$, error bars = SEM. (**D**) Differential effect of soluble and WT Sdc1 on breast cancer cell proliferation. Control vector-transfected MCF-7 and MCF-7 cells stably overexpressing WT (Sdc1-WT), constitutively membrane-bound (Sdc1-388) or the soluble ectodomain of Sdc1 were subjected to an Alamar Blue cell proliferation assay for 6 h. $^{*}P < 0.05$, $n \geq 3$, error bars = SEM.

functional properties of the overexpressed Sdc1 constructs. In addition, we observed an occasional perinuclear and/or nuclear staining for Sdc1. While the perinuclear staining may be indicative of high biosynthetic activity in the ER of the syndecan-overexpressing cell lines, the nuclear localization is conform with reports on a cotrafficking of syndecans with nuclear FGF-2 in injured neurons (40) and on tubulin-mediated nuclear translocation of Sdc1 (41). Although speculative, nuclear trafficking of Sdc1 may exert an influence on cell-cycle progression or on FGF2-mediated transcriptional regulation.

We demonstrated extensive glycosaminoglycan substitution of the heterologously expressed Sdc1 constructs (Figure 1E), which is a prerequisite for their HS-dependent functions, as a multitude of ligands functionally interact with Sdc1 via its HS chains (1,3). Disaccharide analysis revealed the presence of very similar HS structures in the different MCF-7 transfectants. A slightly reduced overall sulfation was noted in MCF-7 Sdc1 392CS cells, yet unchanged levels of trisulfated disacharides. Reduced 6-*O*-sulfation can influence growth factor binding by HS (42), as recently shown for the MCF-7-derived HS-editing enzyme HSulf-2 (43). Therefore, we cannot fully exclude a partial contribution of reduced HS sulfation to the phenotype of MCF-7 Sdc1 392CS cells. The presence of unchanged amounts of trisulfated disaccharides together with the notion that much more HS was produced in these cells (data not shown) may suggest a high ligand-binding capacity also in these cells.

Our coimmunolocalization data suggest that in cells overexpressing the uncleavable Sdc1 mutant, endogenous Sdc1 may also become resistant to shedding, possibly due to heterodimer formation (5,10). A cell rounding upon soluble Sdc1 ectdomain overexpression (Figure 1C panel Sdc1 392CS) has previously been attributed to β1-integrin activation (44); however, focal adhesion formation was not impaired (Figure 4C; supplementary Figure 1 is available at *Carcinogenesis* Online). Moreover, no significantly different alphaV- and β5-integrin expression was observed, consistent with reports on the lack of an inhibitory effect of Sdc1 on αVβ1-integrin-dependent spreading and of Sdc1 inhibiton on MCF-7 migration through vitronectin- and fibronectin-coated filters (13).

Sdc1 siRNA knockdown caused significantly decreased FGF-2-induced MAPK activation (Figure 2), in accordance with its coreceptor role for FGF-2 signaling (1,31). In MCF-7 cells, Sdc1 and -4 contribute to the formation of a ternary complex of FGF-2, FGFR-1 and the syndecans' HS chains (45). In line with the inhibitory effect of Sdc1 knockdown on mitogenic signaling, overexpression of WT Sdc1

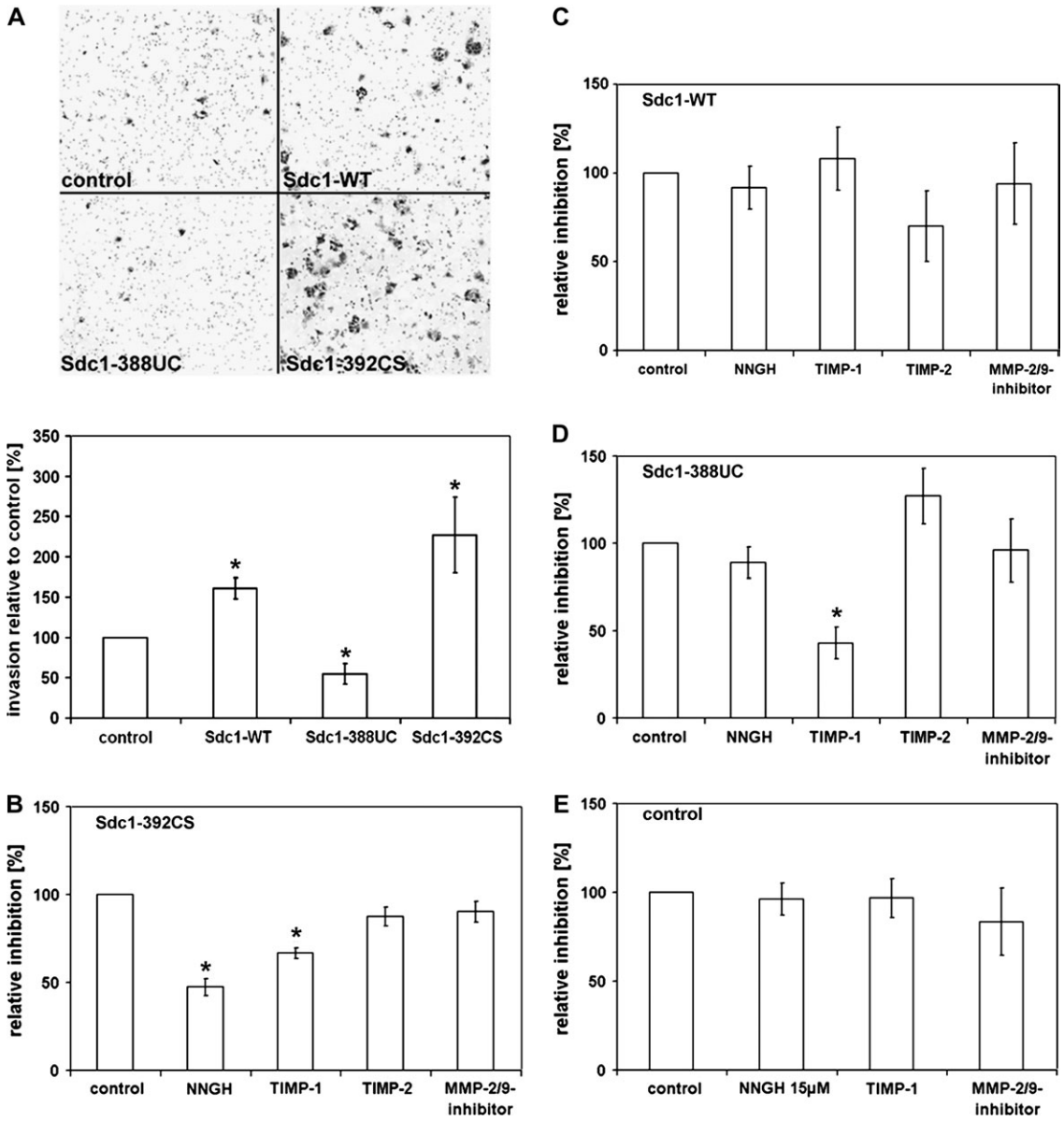

Fig. 3. Differential role of membrane-bound and soluble forms of Sdc1 on TIMP-1-sensitive breast cancer cell invasion. (**A**) Stably transfected MCF-7 cells were subjected to a matrigel invasion assay. Upper panel: representative image of bottom surface of matrigel matrix filters stained with Diff-Quik dye. Lower panel: quantification of invasive cells relative to control vector-transfected cells. (**B–D**) Differential sensitivity of stably transfected MCF-7 cells to a spectrum of MMP inhibitors in the invasion assay. MCF-7 transfectants were subjected for 48 h to an invasion assay in the absence or presence of the broad spectrum MMP/ADAM inhibitor *N*-isobutyl-*N*-(4-methoxyphenylsulfonyl) glycyl hydroxamic acid (NNGH) (1.5/15 μM), TIMP-1 (3.5 nM), TIMP-2 (10 nM) or an MMP-2/MMP9-inhibitor (1 μM). $^{*}P < 0.05$, $n \geq 5$, error bars = SEM

increased the number of coreceptors at the cell surface, resulting in increased cell proliferation rates (Figure 2). In contrast, soluble ectodomain overexpression significantly inhibited MCF-7 proliferation (Figure 2). Soluble Sdc1 inhibits both heparin-binding epidermal growth factor-like growth factor and heparin-mediated FGF-2 mitogenicity (1,32), and exogenously added Sdc1 ectodomains inhibit MCF-7 cell proliferation (28). In turn, FGF-2 induces Sdc1 shedding, providing a mechanism for coreceptor desensitization (30). Decreased TIMP-1 expression (Figure 5) may have additionally reduced MCF-7 Sdc1-392CS cell proliferation since TIMP-1 stimulates MCF-7 cell proliferation via MAPK activation (46,47).

Our study demonstrated that overexpression of WT Sdc1 and its soluble ectodomain significantly promote, whereas the constitutively membrane-bound form inhibits invasiveness of MCF-7 cells (Figure 3). Microarray analysis revealed differential expression of genes involved in proteolytic processes (*TIMP-1*, *uPAR* and *furin*) between highly invasive MCF-7 Sdc1-392CS and control cells. Membrane-bound and soluble Sdc1 differentially modulate proteolytic processes in various experimental systems by targeting different proteins such as elastases, MMP-7, MMP-17 a disintegrin and metalloproteinase with thrombospondin-like motifs-4 and proprotein convertase PC5A (2,15,30,35,48). Our data point to a role for differential TIMP-1 expression as a relevant proinvasive factor in MCF-7 Sdc1-392CS cells and an anti-invasive factor in MCF-7 Sdc1-388UC cells since TIMP-1 secretion was either downregulated or upregulated in these cells. Moreover, addition of TIMP-1 to the culture medium of MCF-7 Sdc1-392CS cells significantly inhibited the increased invasiveness. The preferential inhibitory effect of *N*-isobutyl-*N*-(4-methoxyphenylsulfonyl) glycyl hydroxamic acid may indicate an important role of a disintegrin and metalloproteinases (ADAMs) in this process, conform with the role of ADAM10 in E-cadherin shedding (49) and the observed downregulation of E-cadherin levels (Figure 5A). TIMP-1

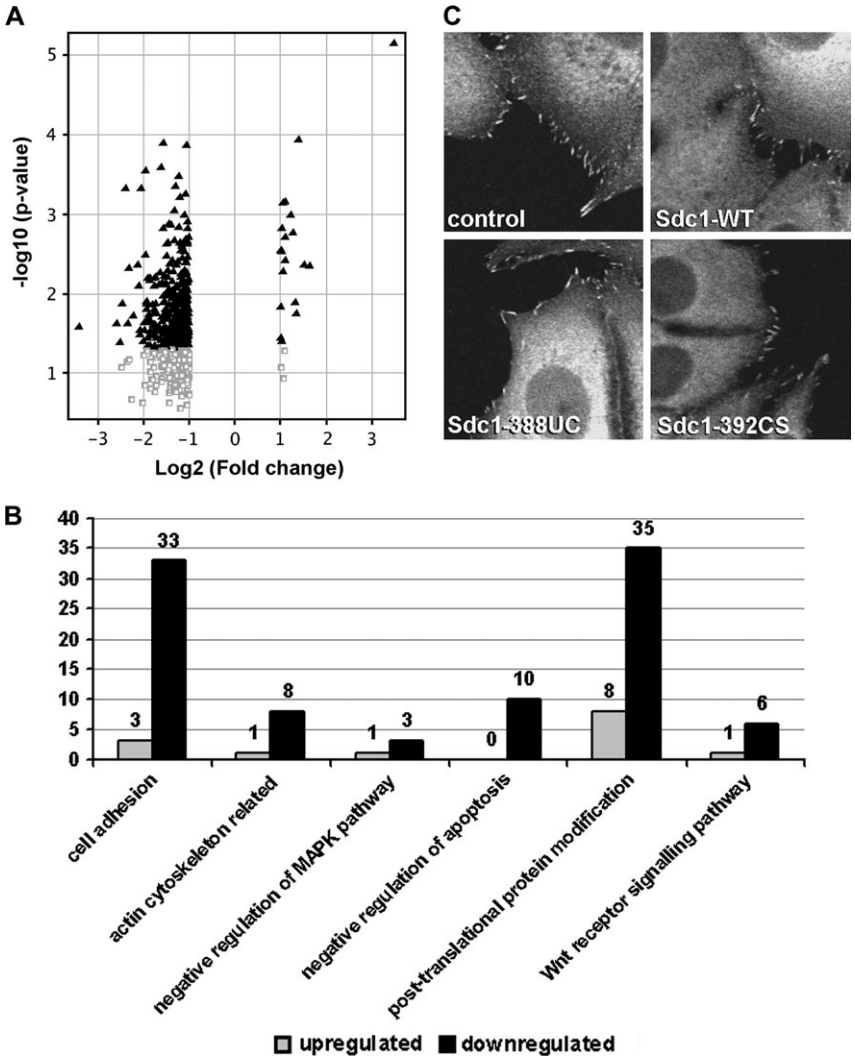

Fig. 4. Affymetrix microarray analysis for differential gene expression between control and highly invasive MCF-7 cells overexpressing soluble Sdc1. mRNA was isolated from control vector and MCF-7 Sdc1-392CS cells, transcribed into complementary DNA and subjected to an Affymetrix microarray analysis (see text and supplementary Tables I–III, available at *Carcinogenesis* Online, for further details). Differentially expressed genes were selected based on the following criteria for the logged data: ($E_{mean} - B_{mean}$) > 1 or (B_{mean}–E_{mean}) > 1 [where E = experiment (Sdc1-392CS), B = baseline (control)]; present call percentage of $E \geq 0$ and present call percentage of $B \geq 100$ or vice versa; unpaired t-test $P < 0.05$. (**A**) Volcano plot of genes with at least a 2-fold change in expression levels in the Sdc1-392CS group compared against control vector-transfected cells, with $P < 0.05$ (black triangles). Genes with P-values >0.05 are shown as gray squares (c.f. supplementary Tables I and II, available at *Carcinogenesis* Online, for gene list). (**B**) Gene Ontology groupings of upregulated and downregulated genes detected in the Affymetrix microarray screen that have known functions relevant to the observed phenotypic changes (c.f. supplementary Table III is available at *Carcinogenesis* Online). (**C**) Confocal immunofluorescence microscopic analysis of heterologously expressed Sdc1 and the focal adhesion protein vinculin in MCF-7 cells grown on a fibronectin substrate (c.f. supplementary Figure 1, available at *Carcinogenesis* Online, for color separation figure of Sdc1/vinculin costaining).

inhibits the proteolytic activity of (non-MT-) MMPs and some ADAMs (ADAM10 and a disintegrin and metalloproteinase with thrombospondin-like motifs) via non-covalent binding to both active and pro-forms of these enzymes (47,50,51). Surprisingly, TIMP-1 did not reduce invasiveness of MCF-7 Sdc1-WT cells. This finding suggests a regulatory function of the equilibrium between membrane-bound and soluble forms of Sdc1. The observed Sdc1-induced changes in TIMP-1 expression and susceptibility are probably based on alterated signaling processes, as suggested by the effect of Sdc1 siRNA knockdown on MAPK signaling (Figure 2C), and by the differential regulation of several members of the MAPK family (*MAP3K8* and *MAP2K*), and upstream signaling molecules (*EGF receptor ERBB2*, *epidermal growth factor receptor pathway substrate 15-like 1* and *integrin-linked kinase*) observed in the Affymetrix screening (supplementary Tables I and II are available at *Carcinogenesis* Online). In turn, TIMP-1 modulates MAPK signaling in MCF-7 cells (46,47). We can currently only speculate that overexpression of either the soluble or membrane-bound form of Sdc1 leads to an activation of pathways modulating TIMP-1 expression and susceptibility, whereas these parameters remain stable if the homeostasis between the two Sdc1 forms is intact.

Upregulation of the prognostic factor uPAR (52) in MCF-7 Sdc1-392CS cells was identified as an additional element contributing to increased invasiveness (Figure 5). uPA binds to its receptor uPAR, thereby enhancing its ability to activate plasmin (52). This provides a potent protease capable of degrading most components of extracellular matrix. Like Sdc1, uPAR indirectly regulates cell adhesion and motility via modulation of αvβ3 integrin function (13). PMA-induced uPAR upregulation in MCF-7 cells causes increased plasminogen binding and activation (53), concomitant with increased Sdc1 shedding (Figure 1C panel Sdc1 388UC). Anti-uPAR antibodies suppress tumor growth and metastasis in MCF-7 xenograft models (52). Furthermore, stromal derived factor (SDF)-1/CXC chemokine receptor 4-mediated upregulation of uPAR in breast cancer cells promotes

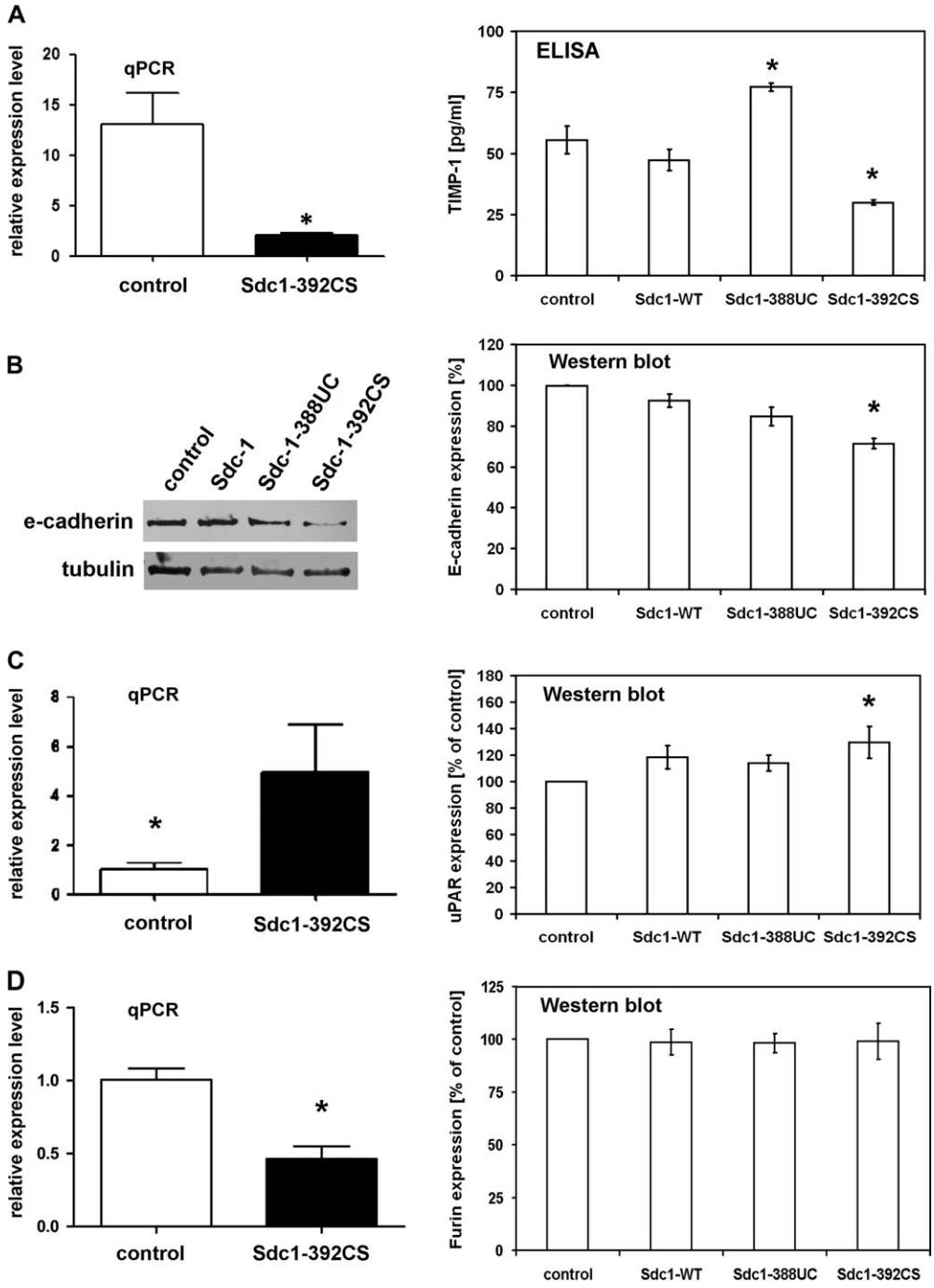

Fig. 5. Dysregulation of TIMP-1, E-cadherin, uPAR and furin expression in MCF-7 cells overexpressing soluble Sdc1. (**A**) Left panel: quantitative PCR analysis of TIMP-1 expression reveals TIMP-1 mRNA downregulation in Sdc1-392CS-transfected MCF-7 cells compared with vector controls. $^{*}P < 0.05$, $n = 3$, error bars = SEM. Right panel: enzyme-linked immunosorbent assay for TIMP-1 protein expression in serum-free cell culture supernatants of stably transfected MCF-7 cells subjected to matrigel invasion assays. Cells overexpressing soluble Sdc1 (Sdc1-392CS) show decreased, and cells overexpressing constitutively membrane-bound Sdc1 (Sdc1-388UC) show increased expression and secretion of TIMP-1 relative to vector controls. $^{*}P < 0.05$, $n \geq 3$, error bars = SEM. (**B**) Western blot for E-cadherin expression in Sdc1-transfected MCF-7 cells. Left panel: picture of a representative experiment. Right panel: densitometric analysis of three independent experiments. E-cadherin expression is significantly decreased upon overexpression of soluble Sdc1. $^{*}P < 0.05$, $n = 3$, error bars = SEM. (**C**) Left panel: quantitative PCR analysis of urokinase-type plasminogen activator receptor expression reveals uPAR mRNA upregulation in Sdc1-392CS-transfected MCF-7 cells compared with vector controls. $^{*}P < 0.05$, $n = 3$, error bars = SEM. Right panel: western blot for uPAR expression in Sdc1-transfected MCF-7 cells. Densitometric analysis of 10 independent experiments reveals significantly increased uPAR expression upon overexpression of soluble Sdc1. $^{*}P < 0.05$, $n = 10$, error bars = SEM. (**D**) Left panel: quantitative PCR analysis of furin expression reveals transcriptional downregulation in Sdc1-392CS-transfected MCF-7 cells compared with vector controls. $^{*}P < 0.05$, $n = 3$, error bars = SEM. Right panel: western blot analysis reveals no changes in furin protein expression between Sdc1-transfected MCF-7 cells. Error bars = SEM.

invasion *in vitro* (54). Like PMA, SDF-1 induces upregulation of uPAR and Sdc1 shedding (12) resulting in increased proteolysis and cancer cell invasiveness.

Finally, downregulation of E-cadherin protein expression was identified as a contributing factor to increased invasiveness of MCF-7 Sdc1-392CS cells (Figure 5). Reduced E-cadherin expression in

breast cancer is associated with lymph node metastasis and reduced disease-free survival (55,56). Sdc1 and E-cadherin are co-ordinately regulated [c.f. (19) for discussion] and coimmunoprecipitate with the transcriptional regulator β-catenin, suggesting functional and physical association (6). Since E-cadherin, like Sdc1, is required for maintaining the epitheloid phenotype (1,55), its downregulation in soluble Sdc1-overexpressing cells facilitates loosening of cell–cell contacts, thus promoting invasiveness. Affymetrix data on the downregulation of 33 genes involved in cell adhesion support this mechanistic concept (Figure 4B).

In summary, we have demonstrated opposing roles for membrane-bound and soluble forms of Sdc1 in human MCF-7 breast cancer cells. In MCF-7 cells, WT Sdc1 promoted cell proliferation as a coreceptor of mitogenic MAPK signaling, whereas its soluble form inhibited proliferation. In contrast, the constitutively membrane-bound form inhibited *in vitro* invasiveness, whereas soluble Sdc1 vastly promoted MCF-7 invasion. Among the multitude of established human breast cancer cell lines, MCF-7 cells represent the more benign spectrum (57). Therefore, the observed Sdc1-induced phenotype may not be representative for all breast cancer cells and may be modulated by the cell-type-specific expression signature of additional receptors, adhesion molecules, growth factors and proteases (19). Microarray analysis revealed that overexpression of soluble Sdc1 was associated with complex changes in the expression pattern of nearly 400 gene products, among which the modulation of proteolytic activity and signal transduction pathways emerged as important motifs relevant to the observed phenotypic changes (Figure 3, Table I; supplementary Tables I–III are available at *Carcinogenesis* Online). Although dysregulation of RhoB was not confirmed in an independent data set (Table I), the large number of differentially regulated Rho-family guanosine triphosphatases (RhoB, RhoC, RhoD and Cdc42) of associated regulatory proteins (Rho-related BTB domain 3, Rho guanine nucleotide exchange factor and SLIT-ROBO Rho GTPase activating protein) and of cytoskeletal elements (smoothelin, alpha actinin and transgelin) identified by Affymetrix screening is highly suggestive of a mechanistic contribution of soluble Sdc1 to the modulation of cell motility as part of the invasion phenotype (supplementary Tables I–III are available at *Carcinogenesis* Online). This view is supported by an increasing number of reports on the interplay of syndecans and Rho-family guanosine triphosphatases (reviewed in ref. 14) and warrants future investigation. We confirmed a coreceptor role for Sdc1 in MAPK-mediated signaling in breast cancer cells and a role for soluble Sdc1 in the regulation of TIMP-1, uPAR and E-cadherin expression, resulting in synergistic promotion of breast cancer cell invasiveness. We propose that TIMP-1-sensitive protease-mediated shedding of Sdc1, mimicked by the Sdc1-392CS expression construct, represents a switch from a proliferative to an invasive phenotype in MCF-7 cells. This model is able to explain seemingly contradictory results on the prognostic role of Sdc1 in breast cancer (18,22–24). In histopathological analyses, soluble Sdc1 may have been lost during sample preparation. Therefore, specimens regarded as Sdc1 negative due to low membranous epithelial staining may in fact represent a tumor subtype with a high potential to metastasize. Our findings also have a therapeutic perspective, considering that the major functional domains of soluble Sdc1 are its heparin-related HS chains. In early stages of tumor progression, competitive glycosaminoglycan-based approaches targeting the interaction of growth factors with Sdc1 emerge as a promising anti-proliferative strategy. In contrast, some glycosaminoglycans may potentially mimic the soluble Sdc1 ectodomain and may promote rather than inhibit metastasis at later stages of cancer progression. Heparanase induces Sdc1 expression and shedding, which promotes tumor invasion (58). Therefore, the combined use of Sdc1 shedding inhibitors, MMP inhibitors and heparanase-inhibiting heparinoids may be a promising anti-metastatic approach at late stages of breast cancer progression (8,59). The results of our study therefore underline the importance of a mechanistic understanding of the biological roles of prognostic markers for the development of targeted therapeutic approaches.

Supplementary materials

Supplementary Tables I–III and Figures 1 and 2 can be found at http://carcin.oxfordjournals.org/

Funding

Deutsche Forschungsgemeinschaft (DFG GÖ1392 1-2 to M.G.); National Medical Research Council, Singapore (NMRC/1023/2005 to G.W.Y.); German Academic Exchange service (DAAD A/06/90277 to S.A.I.); Graduate Research Scholarship, National University of Singapore to C.-Y.K.

Acknowledgements

We thank Birgit Pers, Eng-Siang Yong, Siew-Hua Choo and Ruth Goez for their excellent technical assistance.

Conflict of Interest Statement: None declared.

References

1. Bernfield,M. *et al*. (1999) Functions of cell surface heparan sulfate proteoglycans. *Annu. Rev. Biochem.*, **68**, 729–777.
2. Elenius,V. *et al*. (2004) Inhibition by the soluble syndecan-1 ectodomains delays wound repair in mice overexpressing syndecan-1. *J. Biol. Chem.*, **279**, 41928–41935.
3. Götte,M. (2003) Syndecans in inflammation. *FASEB J.*, **17**, 575–591.
4. McDermott,S.P. *et al*. (2007) Juvenile syndecan-1 null mice are protected from carcinogen-induced tumor development. *Oncogene*, **26**, 1407–1416.
5. Dews,I.C. *et al*. (2007) Transmembrane domains of the syndecan family of growth factor coreceptors display a hierarchy of homotypic and heterotypic interactions. *Proc. Natl Acad. Sci. USA*, **104**, 20782–20787.
6. Zimmermann,P. *et al*. (2001) Characterization of syntenin, a syndecan-binding PDZ protein, as a component of cell adhesion sites and microfilaments. *Mol. Biol. Cell*, **12**, 339–350.
7. McQuade,K.J. *et al*. (2003) Syndecan-1 transmembrane and extracellular domains have unique and distinct roles in cell spreading. *J. Biol. Chem.*, **278**, 46607–46615.
8. Yip,G.W. *et al*. (2006) Therapeutic value of glycosaminoglycans in cancer. *Mol. Cancer Ther.*, **5**, 2139–2148.
9. Langford,J.K. *et al*. (2005) Identification of an invasion regulatory domain within the core protein of syndecan-1. *J. Biol. Chem.*, **280**, 3467–3473.
10. Wang,Z. *et al*. (2005) Constitutive and accelerated shedding of murine syndecan-1 is mediated by cleavage of its core protein at a specific juxtamembrane site. *Biochemistry*, **44**, 12355–12361.
11. Endo,K. *et al*. (2003) Cleavage of syndecan-1 by membrane type matrix metalloproteinase-1 stimulates cell migration. *J. Biol. Chem.*, **278**, 40764–40770.
12. Brule,S. *et al*. (2006) The shedding of syndecan-4 and syndecan-1 from HeLa cells and human primary macrophages is accelerated by SDF-1/CXCL12 and mediated by the matrix metalloproteinase-9. *Glycobiology*, **16**, 488–501.
13. Beauvais,D.M. *et al*. (2004) The syndecan-1 ectodomain regulates alphavbeta3 integrin activity in human mammary carcinoma cells. *J. Cell Biol.*, **167**, 171–181.
14. Morgan,M.R. *et al*. (2007) Synergistic control of cell adhesion by integrins and syndecans. *Nat. Rev. Mol. Cell Biol.*, **8**, 957–969.
15. Vanhoutte,D. *et al*. (2007) Increased expression of syndecan-1 protects against cardiac dilatation and dysfunction after myocardial infarction. *Circulation*, **115**, 475–482.
16. Rops,A.L. *et al*. (2007) Syndecan-1 deficiency aggravates anti-glomerular basement membrane nephritis. *Kidney Int.*, **72**, 1204–1215.
17. Maeda,T. *et al*. (2006) Syndecan-1 expression by stromal fibroblasts promotes breast carcinoma growth *in vivo* and stimulates tumor angiogenesis. *Oncogene*, **25**, 1408–1412.
18. Baba,F. *et al*. (2006) Syndecan-1 and syndecan-4 are overexpressed in an estrogen receptor-negative, highly proliferative breast carcinoma subtype. *Breast Cancer Res. Treat.*, **98**, 91–98.
19. Götte,M. *et al*. (2007) An expression signature of syndecan-1 (CD138), E-cadherin and c-met is associated with factors of angiogenesis and lymphangiogenesis in ductal breast carcinoma *in situ*. *Breast Cancer Res.*, **9**, R8.
20. Hill,R.P. *et al*. (2007) ''Destemming'' cancer stem cells. *J. Natl Cancer Inst.*, **99**, 1435–1440.

21. Götte,M. *et al*. (2006) Predictive value of syndecan-1 expression for the response to neoadjuvant chemotherapy of primary breast cancer. *Anticancer Res.*, **26**, 621–627.
22. Barbareschi,M. *et al*. (2003) High syndecan-1 expression in breast carcinoma is related to an aggressive phenotype and to poorer prognosis. *Cancer*, **98**, 474–483.
23. Leivonen,M. *et al*. (2004) Prognostic value of syndecan-1 expression in breast cancer. *Oncology*, **67**, 11–18.
24. Berton-Rigaud,D. *et al*. (2008) Prognostic impact of syndecan-1 expression in invasive ductal breast carcinomas. *Br. J. Cancer*, **98**, 1993–1998.
25. Sonntag,B. *et al*. (2005) Metformin alters insulin signalling and viability of human granulosa cells. *Fertil. Steril.*, **84** (suppl. 2), 1173–1179.
26. Guo,C.H. *et al*. (2007) Comparison of the effects of differentially sulphated bovine kidney- and porcine intestine-derived heparan sulphate on breast carcinoma cellular behaviour. *Int. J. Oncol.*, **31**, 1415–1423.
27. Li,C. *et al*. (2001) Model-based analysis of oligonucleotide arrays: expression index computation and outlier detection. *Proc. Natl Acad. Sci. USA*, **98**, 31–36.
28. Ledin,J. *et al*. (2004) Heparan sulfate structure in mice with genetically modified heparan sulfate production. *J. Biol. Chem.*, **279**, 42732–42741.
29. Mali,M. *et al*. (1994) Suppression of tumor cell growth by syndecan-1 ectodomain. *J. Biol. Chem.*, **269**, 27795–27798.
30. Su,G. *et al*. (2007) Shedding of syndecan-1 by stromal fibroblasts stimulates human breast cancer cell proliferation via FGF2 activation. *J. Biol. Chem.*, **282**, 14906–14915.
31. Steinfeld,R. *et al*. (1996) Stimulation of fibroblast growth factor receptor-1 occupancy and signaling by cell surface-associated syndecans and glypican. *J. Cell Biol.*, **133**, 405–416.
32. Kato,M. *et al*. (1998) Physiological degradation converts the soluble syndecan-1 ectodomain from an inhibitor to a potent activator of FGF-2. *Nat. Med.*, **4**, 691–697.
33. Forsten,K.E. *et al*. (1997) Endothelial proteoglycans inhibit bFGF binding and mitogenesis. *J. Cell. Physiol.*, **172**, 209–220.
34. Kaushal,G.P. *et al*. (1999) Syndecan-1 expression suppresses the level of myeloma matrix metalloproteinase-9. *Br. J. Haematol.*, **104**, 365–373.
35. Gao,G. *et al*. (2004) ADAMTS4 (aggrecanase-1) activation on the cell surface involves C-terminal cleavage by glycosylphosphatidyl inositol-anchored membrane type 4-matrix metalloproteinase and binding of the activated proteinase to chondroitin sulfate and heparan sulfate on syndecan-1. *J. Biol. Chem.*, **279**, 10042–10051.
36. Bertini,I. *et al*. (2004) Crystal structure of the catalytic domain of human matrix metalloproteinase 10. *J. Mol. Biol.*, **336**, 707–716.
37. Arendt,Y. *et al*. (2007) Catalytic domain of MMP20 (Enamelysin)—the NMR structure of a new matrix metalloproteinase. *FEBS Lett.*, **581**, 4723–4726.
38. MacPherson,L.J. *et al*. (1997) Discovery of CGS 27023A, a non-peptidic, potent, and orally active stromelysin inhibitor that blocks cartilage degradation in rabbits. *J. Med. Chem.*, **40**, 2525–2532.
39. Ashburner,M. *et al*. (2000) Gene ontology: tool for the unification of biology. The Gene Ontology Consortium. *Nat. Genet.*, **25**, 25–29.
40. Leadbeater,W.E. *et al*. (2006) Intracellular trafficking in neurones and glia of fibroblast growth factor-2, fibroblast growth factor receptor 1 and heparan sulphate proteoglycans in the injured adult rat cerebral cortex. *J. Neurochem.*, **96**, 1189–1200.
41. Brockstedt,U. *et al*. (2002) Immunoreactivity to cell surface syndecans in cytoplasm and nucleus: tubulin-dependent rearrangements. *Exp. Cell Res.*, **274**, 235–245.
42. Lamanna,W.C. *et al*. (2008) Sulf loss influences N-, 2-O-, and 6-O-sulfation of multiple heparan sulfate proteoglycans and modulates fibroblast growth factor signaling. *J. Biol. Chem.*, **283**, 27724–27735.
43. Uchimura,K. *et al*. (2006) HSulf-2, an extracellular endoglucosamine-6-sulfatase, selectively mobilizes heparin-bound growth factors and chemokines: effects on VEGF, FGF-1, and SDF-1. *BMC Biochem.*, **7**, 2.
44. Burbach,B.J. *et al*. (2004) Syndecan-1 ectodomain regulates matrix-dependent signaling in human breast carcinoma cells. *Exp. Cell Res.*, **300**, 234–247.
45. Mundhenke,C. *et al*. (2002) Heparan sulfate proteoglycans as regulators of fibroblast growth factor-2 receptor binding in breast carcinomas. *Am. J. Pathol.*, **160**, 185–194.
46. Porter,J.F. *et al*. (2004) Tissue inhibitor of metalloproteinase-1 stimulates proliferation of human cancer cells by inhibiting a metalloproteinase. *Br. J. Cancer*, **90**, 463–470.
47. Würtz,S.Ø. *et al*. (2005) Tissue inhibitor of metalloproteinases-1 in breast cancer. *Endocr. Relat. Cancer*, **12**, 215–227.
48. Mayer,G. *et al*. (2008) The regulated cell surface zymogen activation of the proprotein convertase PC5A directs the processing of its secretory substrates. *J. Biol. Chem.*, **283**, 2373–2384.
49. Maretzky,T. *et al*. (2005) ADAM10 mediates E-cadherin shedding and regulates epithelial cell-cell adhesion, migration, and beta-catenin translocation. *Proc. Natl Acad. Sci. USA*, **102**, 9182–9187.
50. Duffy,M.J. *et al*. (2000) Metalloproteinases: role in breast carcinogenesis, invasion and metastasis. *Breast Cancer Res.*, **2**, 252–257.
51. Egeblad,M. *et al*. (2002) New functions of the matrix metalloproteinases in cancer progression. *Nat. Rev. Cancer*, **2**, 161–174.
52. Rasch,M.G. *et al*. (2008) Intact and cleaved uPAR forms: diagnostic and prognostic value in cancer. *Front. Biosci.*, **13**, 6752–6762.
53. Stillfried,G.E. *et al*. (2007) Plasminogen binding and activation at the breast cancer cell surface: the integral role of urokinase activity. *Breast Cancer Res.*, **9**, R14.
54. Serratì,S. *et al*. (2008) Endothelial cells and normal breast epithelial cells enhance invasion of breast carcinoma cells by CXCR-4-dependent up-regulation of urokinase-type plasminogen activator receptor (uPAR, CD87) expression. *J. Pathol.*, **214**, 545–554.
55. Cowin,P. *et al*. (2005) Cadherins and catenins in breast cancer. *Curr. Opin. Cell Biol.*, **17**, 499–508.
56. Jones,J.L. *et al*. (1996) E-cadherin relates to EGFR expression and lymph node metastasis in primary breast carcinoma. *Br. J. Cancer*, **74**, 1237–1241.
57. Lacroix,M. *et al*. (2004) Relevance of breast cancer cell lines as models for breast tumours: an update. *Breast Cancer Res. Treat.*, **83**, 249–289.
58. Yang,Y. *et al*. (2007) Heparanase enhances syndecan-1 shedding: a novel mechanism for stimulation of tumor growth and metastasis. *J. Biol. Chem.*, **282**, 13326–13333.
59. Götte,M. *et al*. (2006) Heparanase, hyaluronan, and CD44 in cancers: a breast carcinoma perspective. *Cancer Res.*, **66**, 10233–10237.

Received June 24, 2008; revised November 9, 2008; accepted December 21, 2008